

ASCA OBSERVATION OF AN X-RAY–LUMINOUS ACTIVE NUCLEUS IN MARKARIAN 231

PHILIP R. MALONEY

Center for Astrophysics and Space Astronomy, University of Colorado, Campus Box 389,
Boulder, CO 80309-0389; maloney@casa.colorado.edu

AND

CHRISTOPHER S. REYNOLDS¹

JILA, University of Colorado, Campus Box 440, Boulder, CO 80309-0440; chris@rocinate.colorado.edu

Received 2000 July 13; accepted 2000 October 4; published 2000 November 21

ABSTRACT

We have obtained a moderately long (10^5 s) *ASCA* observation of the Seyfert 1 galaxy Markarian 231, the most luminous of the local ultraluminous infrared galaxy population. In the best-fitting model we do not see the X-ray source directly; the spectrum consists of a scattered power-law component and a reflection component, both of which have been absorbed by a column $N_{\text{H}} \approx 3 \times 10^{22}$ cm⁻². About three-quarters of the observed hard X-rays arise from the scattered component, reducing the equivalent width of the iron $K\alpha$ line. The implied ratio of 1–10 keV X-ray luminosity to bolometric luminosity, $L_{\text{X}}/L_{\text{bol}} \sim 2\%$, is typical of Seyfert 1 galaxies and radio-quiet QSOs of comparable bolometric luminosities and indicates that the bolometric luminosity is dominated by the active galactic nucleus (AGN). Our estimate of the X-ray luminosity also moves Mrk 231 in line with the correlations found for AGNs with extremely strong Fe II emission. A second source separated by about $2'$ is also clearly detected and contributes about 25% of the total flux.

Subject headings: galaxies: active — galaxies: individual (Markarian 231) — galaxies: nuclei — galaxies: Seyfert — X-rays: galaxies

1. INTRODUCTION

Sixteen years ago, the *IRAS* all-sky survey revealed the existence of a class of objects which emit nearly all of their energy at far-infrared wavelengths (Soifer et al. 1984). At the high-luminosity end of the distribution, $L_{\text{IR}} \geq 10^{12} L_{\odot}$, the so-called ultraluminous infrared galaxies (ULIRGs), the space density of such objects is approximately twice that of optically selected QSOs, the only objects with comparable bolometric luminosities (Sanders & Mirabel 1996). The far-infrared energy distributions of the prototype objects, Arp 220 and NGC 6240, are very similar to that of the classic starburst galaxy M82, peaking at $\lambda \approx 60$ μm , and do not exhibit the “warm” *IRAS* colors typical of Seyfert galaxies (DeGrijs et al. 1992). A large fraction of the ultraluminous galaxies show evidence for interaction or merging with a companion galaxy (Sanders et al. 1988; Melnick & Mirabel 1990), and most show luminous molecular line emission, indicating substantial quantities of molecular gas, which could potentially fuel either a burst of star formation or an active galactic nucleus (AGN; e.g., Sanders & Mirabel 1996 and references therein).

Ever since the discovery of this class of galaxies, debate has raged over the nature of the dominant source of energy. The failure to detect any of the ULIRGs at X-ray wavelengths with *HEAO 1* (Rieke 1988) strengthened a starburst interpretation, as did the recent failure of the OSSE instrument on the *Gamma Ray Observatory* to detect Arp 220, Mrk 231, or Mrk 273 in the 50–200 keV energy range (Dermer et al. 1997); this rules out very luminous Compton-thin sources in these galaxies. Most recently, observations of a number of ULIRGs with the short-wavelength spectrometer on the *Infrared Space Observatory* failed to detect any high-excitation lines in the mid-infrared, as might be expected from even a dust-shrouded AGN (Sturm et al. 1996; Genzel et al. 1998), and this has been taken to be evidence for starbursts rather than AGNs. However, it is

now clear that in many ULIRGs the column densities toward the nucleus are so high that the dust optical depth is greater than unity even in the mid-IR. Furthermore, the discovery of Compton-thick X-ray sources in a number of ULIRGs, notably including NGC 6240 (Iwasawa & Comastri 1998; Vignati et al. 1999), substantially weakens the argument against AGN-dominated sources based on hard X-ray nondetections. Such sources, in which even hard X-rays are seen only through reflection, are characterized by a relatively flat continuum above $E \sim 3$ keV and very large equivalent widths of the iron $K\alpha$ line, exceeding 1 keV (e.g., Krolik & Kallman 1987; Krolik, Madau, & Życki 1994; Matt, Brandt, & Fabian 1996). Such large equivalent widths can be produced only if the X-ray continuum incident on the line-emitting region is much larger than that which we observe. If the reflected fraction in NGC 6240 is similar to that in NGC 1068, the bolometric luminosity of the AGN is of order 10^{45} ergs s⁻¹ and dominates the far-infrared output of the galaxy.

Foremost among the local ULIRGs is Markarian 231 ($z = 0.042$), which is the most luminous object in the local universe ($z < 0.1$; Soifer et al. 1984). Its bolometric luminosity is $L_{\text{bol}} \approx 3 \times 10^{12} L_{\odot}$ ($H_0 = 75$ km s⁻¹ Mpc⁻¹), nearly all of which emerges in the far-infrared. Although classified as a Seyfert 1, Mrk 231 shows evidence for substantial amounts of reddening ($A_{\text{V}} \sim 2$; Boksenberg et al. 1977), and when corrected for extinction, its optical luminosity approaches quasar levels. Furthermore, Mrk 231 exhibits many features characteristic of (low-ionization) broad absorption line (BAL) QSOs: high optical polarization (20% at 2800 Å; Smith et al. 1995), strong Fe II emission (extremely strong in Mrk 231; Boksenberg et al. 1977), red optical colors, and a large IR/optical flux ratio. *ASCA* and *ROSAT* observations of Mrk 231, analyzed by Iwasawa (1999) and Turner (1999), revealed an extended, soft X-ray component, with a luminosity $L \sim 10^{42}$ ergs s⁻¹, and a hard component exhibiting considerable absorption, with a 2–10 keV luminosity of only $L \approx 2 \times 10^{42}$ ergs s⁻¹. If this is

¹ Hubble Fellow.

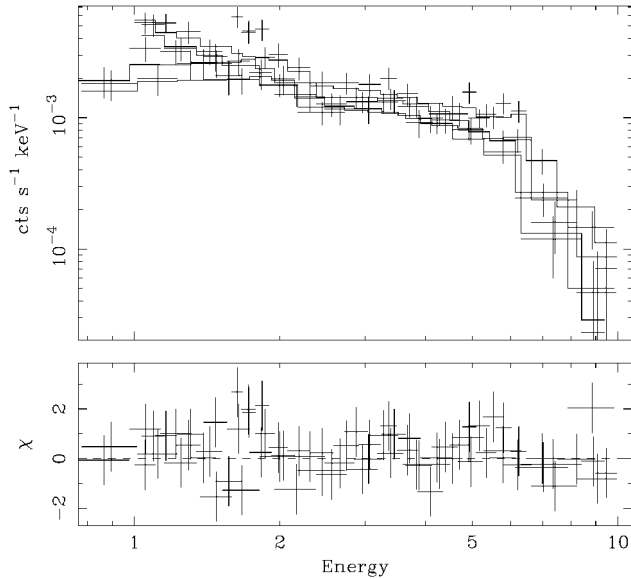


FIG. 1.—ASCA SIS and GIS spectrum of Mrk 231. The top panel shows the data for all four instruments together with the best-fitting folded model (i.e., the model has been folded through the response of the telescope/detector system). The bottom panel shows the contribution of each spectral bin to the overall χ^2 of the best fit.

the intrinsic X-ray luminosity, then an AGN is unlikely to dominate the energetics unless Mrk 231 is X-ray-quiet. However, the signal-to-noise ratio (S/N) of the ASCA spectrum was too low to determine whether the observed X-ray emission is largely reflected, in which case the true X-ray luminosity could be much higher.

In this letter, we present an analysis of a much deeper ASCA observation of Mrk 231 than that presented by Iwasawa (1999). We find strong evidence for a powerful, buried AGN in this ULIRG, which we observe only through reflection and scattering. Indeed, we show that the AGN in Mrk 231 may well be the dominant energy source.

2. OBSERVATION AND DATA REDUCTION

Mrk 231 was observed by ASCA on 1999 November 10. The Solid-State Imaging Spectrometer (SIS) data were cleaned in order to remove the effects of hot and flickering pixels and subjected to the following data-selection criteria: (1) the satellite should not be in the South Atlantic Anomaly (SAA), (2) the object should be at least 7° above the Earth’s limb, (3) the object should be at least 25° above the daytime Earth limb, and (4) the local geomagnetic cutoff rigidity (COR) should be greater than 6 GeV/c. We also applied a standard grade selection on SIS events in order to further minimize particle background. The Gas Imaging Spectrometer (GIS) data were cleaned to remove the particle background and subjected to the following data-selection criteria: (1) the satellite should not be in the SAA, (2) the object should be at least 7° above the Earth’s limb, and (3) the COR should be greater than 7 GeV/c. After these data selection criteria were applied, there were 96.3 ks of good data per SIS detector and 99.2 ks of good data per GIS detector.

Full-band images were extracted from each of the four ASCA detectors. Two pointlike X-ray sources were found in the SIS image separated by $2'$, with the dominant source (containing about 75% of the counts) coincident with Mrk 231. The GIS has insufficient spatial resolution to distinguish these sources.

We extracted the SIS spectrum of each source and found them to have very similar shapes. Given that the fainter source does not dominate at any energy and that detailed spectroscopy on these small scales is difficult due to the energy-dependent point-spread function of ASCA, we chose to extract and analyze the combined spectrum of these sources (which is dominated by Mrk 231).

Source photons were extracted from a circular region centered on the two sources with radii of $3'$ and $4'$ for the SIS and GIS, respectively. Background spectra were obtained from blank regions of the same field (using the same chip in the case of the SIS). No temporal variability was observed. In order to facilitate χ^2 spectral fitting, all spectra were rebinned so as to contain at least 20 photons per spectral bin. In order to avoid poorly calibrated regions of the spectrum, the energy ranges considered were 1.0–10 keV for the SIS detectors and 0.8–10 keV for the GIS detectors. Note that we use a lower energy cutoff for the SIS that is considerably higher than the “standard” 0.6 keV cutoff in order to avoid the effects of “residual dark current distribution,” or RDD, which is known to plague recent ASCA observations.

3. SPECTRAL ANALYSIS

Iwasawa (1999) finds evidence for soft X-ray emission from thermal plasma and measures a temperature of $kT = 0.98_{-0.09}^{+0.51}$ keV and an abundance of $Z = 0.08_{-0.05}^{+0.20} Z_\odot$. Since we deem our soft ($E < 1$ keV) SIS data to be unusable, we cannot constrain the nature of the thermal plasma component. Therefore, in all that follows, we constrain the parameters of the thermal component (kT and Z) to the 90% error range found by Iwasawa.

Guided by Iwasawa (1999), we initially fitted our SIS and GIS spectrum (Fig. 1) with a model consisting of this thermal component and a power-law tail with photon index Γ (representing the AGN emission), all absorbed by the Galactic column of $N_H = 1.26 \times 10^{20} \text{ cm}^{-2}$. Although this spectral model produced an adequate goodness of fit ($\chi^2/\text{degrees of freedom [dof]} = 304/305$), the resulting photon index was extremely flat ($\Gamma = 0.69 \pm 0.12$). In particular, it is much flatter than the intrinsic spectrum (usually $\Gamma = 1.5\text{--}2.2$) of any known AGN. Adding intrinsic absorption to the power-law component increases the permitted photon index by $\Delta\Gamma \sim 0.4$ (with $\Delta\chi^2 = 7$ for one new parameter)—insufficient to bring Γ into the acceptable AGN range.

Since this AGN is likely to be highly obscured, we also examined classes of models in which the central power law is completely absorbed by a Compton-thick screen and is seen only via scattering and Compton reflection. In practice, we used the PEXRAV models within the XSPEC package, interpreting finite reflection fractions as representing mixed reflection/scattering (i.e., scattering of nonreflected as well as reflected continua into our line of sight). A model consisting of this reflected/scattered component and the thermal plasma produced a good fit ($\chi^2/\text{dof} = 284/304$) and implied a reflection-dominated spectrum (with the reflection fraction $\mathcal{R} > 5800$). However, the implied intrinsic power-law was much steeper ($\Gamma = 3.01_{-0.28}^{+0.12}$) than the normal AGN range.

Physically acceptable results are produced when one includes absorption of the reflected/scattered component. While this absorption is not statistically required, including a column of $N_H \sim 3 \times 10^{22} \text{ cm}^{-2}$ extends the range of allowable photon indices into the typical AGN range. In order to better constrain the fits, we hereafter assume that the hard X-ray photon index

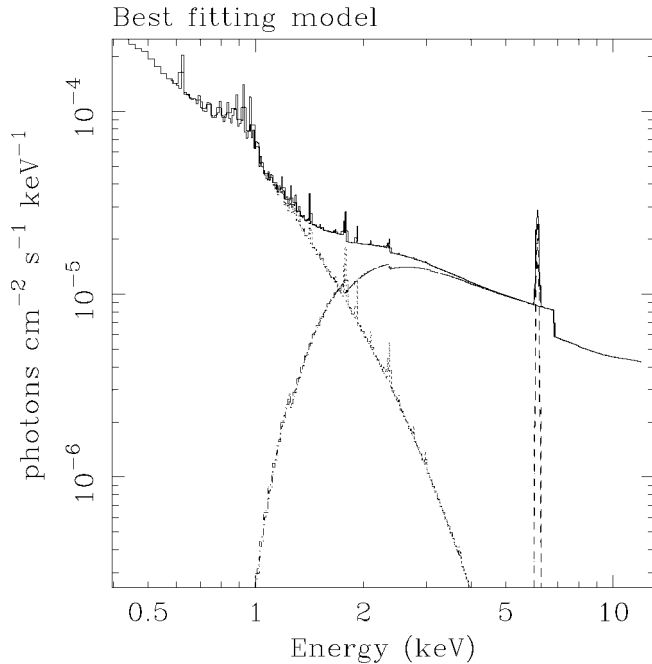


FIG. 2.—Best-fitting spectral model for Mrk 231, plotted in terms of photon flux. Reflected/scattered emission from the AGN component dominates at hard X-ray energies but is truncated at 1–2 keV by heavy neutral absorption. Line-rich thermal plasma spectrum dominates at soft X-ray energies. The strong iron-L complex at ~ 1 keV is clearly visible.

of the source is typical of radio-quiet AGNs, $\Gamma = 1.8$. We also include a narrow iron $K\alpha$ emission line of cold iron, which is expected to accompany the X-ray reflection. The best-fitting parameters (with 90% error range) are then $\mathcal{R} = 8.7_{-5.4}^{+7.9}$, $N_{\text{H}} = 2.9_{-1.0}^{+2.5} \times 10^{22} \text{ cm}^{-2}$, and an iron line equivalent width of $W_{K\alpha} = 290_{-170}^{+190} \text{ eV}$ (with $\chi^2/\text{dof} = 280/303$); the resulting model spectrum is shown in Figure 2. We have experimented with fits assuming partial covering of the source or ionized rather than neutral absorbers; neither the quality nor the nature of the best fits differs in any significant way from the above. This is to be expected since the hard X-ray spectrum largely decouples in the analysis from the soft, absorbed spectrum.

We also investigated the potential presence of an unabsorbed power-law component (corresponding to AGN emission that has been scattered at sufficiently large distances to be free of any substantial absorption). No such component was required by the data, and limits were set on the luminosity of any such component of less than $1.1 \times 10^{42} \text{ ergs s}^{-1}$.

4. DISCUSSION

In his analysis of previous *ASCA* data, Iwasawa (1999) was unable to distinguish between a very flat, unabsorbed power law and a heavily absorbed, typical ($\Gamma = 1.8$) AGN spectrum. With the considerably better S/N provided by our *ASCA* observation, we can show unequivocally that no amount of neutral absorption can steepen the intrinsic photon index into the normal AGN range. We are therefore led to conclude that there is a Compton-thick screen blocking the X-ray source along our line of sight and that we see the AGN only by reflection and scattering of the X-rays into our line of sight (Fig. 3). Furthermore, unless the spectrum of the hard X-ray emission is unusually steep, the reflected/scattered emission is fairly heavily absorbed, by a neutral column $N_{\text{H}} \approx 3 \times 10^{22} \text{ cm}^{-2}$.

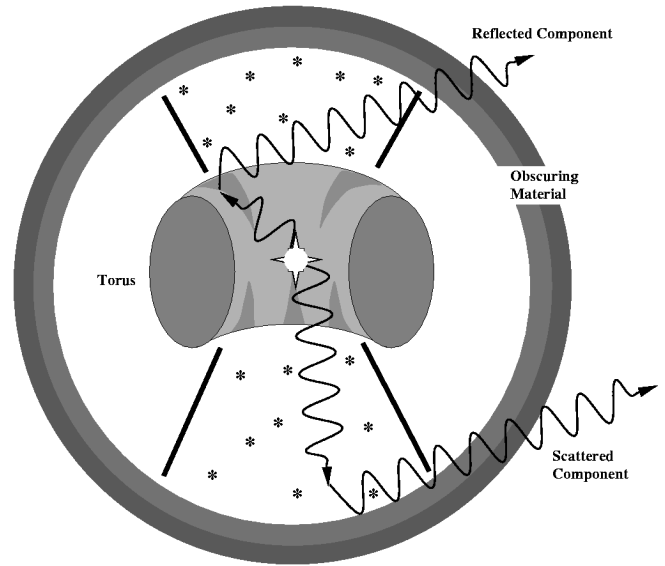


FIG. 3.—Schematic illustration of our inferred geometry for the X-ray emission from Mrk 231, in which we observe only scattered and reflected emission and do not have an unobstructed view of the nucleus and in which there is a distribution of absorbing gas along our line of sight to both the reflected and scattered components of the X-ray emission.

We can estimate the intrinsic luminosity of the X-ray source in two ways. When we subtract the contribution from the thermal emission, the observed 0.5–10 keV luminosity is $2.0 \times 10^{42} \text{ ergs s}^{-1}$. Corrected for neutral absorption, this becomes $3.2 \times 10^{42} \text{ ergs s}^{-1}$, and with the reflection fraction \mathcal{R} set equal to zero, the scattered luminosity is $L_{\text{sc}} = 2.4 \times 10^{42} \text{ ergs s}^{-1}$. (Note that this implies that about three-quarters of the *observed* X-ray luminosity is due to scattering of X-rays into our line of sight, rather than reflection, thus reducing the equivalent width of the Fe $K\alpha$ line from the value of ~ 1 keV expected for a reflection-dominated spectrum.) Hence the intrinsic luminosity of the X-ray source is given by

$$L_{\text{intr}} = 2.4 \times 10^{43} \left(\frac{0.1}{f_{\text{sc}}} \right) \text{ ergs s}^{-1}, \quad (1)$$

where the scattering fraction f_{sc} is expected to be on the order of 1% for electron scattering, assuming that the scattering column density is of the same order as the inferred absorption column density, i.e., a Thompson optical depth of order 0.01.

Alternatively, we can estimate L_{intr} from the reflected fraction and modeling of the reflection process. From the above numbers, the observed luminosity in the reflection component is $L_{\text{refl}} = 8.0 \times 10^{41} \text{ ergs s}^{-1}$. Using XSPEC, we conclude that the product of L_{intr} and the reflection fraction f_{refl} is

$$L_{\text{intr}} f_{\text{refl}} = 2.0 \times 10^{43} \text{ ergs s}^{-1}, \quad (2)$$

and so

$$L_{\text{intr}} = 2.0 \times 10^{44} \left(\frac{0.1}{f_{\text{refl}}} \right) \text{ ergs s}^{-1}, \quad (3)$$

where we have normalized to 0.1 under the assumption that only a small fraction of the reflecting surface is visible to us; for the Compton-thick Seyfert 2 galaxy NGC 1068, Iwasawa, Fabian, & Matt (1997) infer $f_{\text{refl}} \sim 0.05$. These two estimates

of the luminosity agree for a ratio $f_{\text{refl}}/f_{\text{sc}} \approx 10$, i.e., for a reflected fraction $f_{\text{refl}} \approx 0.1$ for a scattered fraction $f_{\text{sc}} \approx 1\%$, which, as noted above, is the value expected if the scattering column is of the same order as the inferred absorbing column. (This ratio of $f_{\text{sc}}/f_{\text{refl}}$ is *not* independent of the value $\mathcal{R} \approx 10$ derived from the spectral fitting.) Thus we infer that $f_{\text{refl}} \approx 0.1$, $f_{\text{sc}} \approx 0.01$, and $L_{\text{X}} \approx 2 \times 10^{44}$ ergs s^{-1} . This is 200 times larger than the value of Iwasawa (1999) and a factor ~ 20 larger than the luminosity estimated by Turner (1999); hence our analysis implies that the AGN is much more X-ray-luminous than previously thought.

From our estimate of the intrinsic hard X-ray luminosity L_{X} , we can estimate the contribution of the AGN to the bolometric luminosity of Mrk 231. The implied ratio of $L_{\text{X}}/L_{\text{bol}} \sim 2\%$. For comparison, the ratio of $L_{\text{X}}/L_{\text{bol}}$ for the Seyfert 1 galaxies and radio-quiet QSOs of the sample of Elvis et al. (1994) for which X-ray data are available ranges from 1.95% to 14.5%. The mean value decreases somewhat with L_{bol} , from 6.3% for $L_{\text{bol}} = 10^{45}$ – 10^{46} (11 objects) to 4.3% for $L_{\text{bol}} = 10^{46}$ to 2.2×10^{46} (seven objects); all the latter are classified as radio-quiet QSOs. Hence, within the uncertainties, the energetics of Mrk 231 are consistent with complete domination by the AGN; in any case, the fraction of the bolometric luminosity contributed by the AGN is almost certainly large (≥ 0.5). Extrapolating to high energies, the predicted 50–200 keV luminosity is $L_{50-200} \approx 2 \times 10^{44}$ ergs s^{-1} , a factor of 5 below the Dermer et al. (1997) upper limit from OSSE.

We also note that with our estimate of the intrinsic X-ray luminosity, Mrk 231 is no longer an outlier in the significant correlations found by Lawrence et al. (1997) in the properties of AGNs with extreme Fe II emission, in particular, those between the 2 keV– $1 \mu\text{m}$ spectral index α_{ix} and the Fe II emission strength and the emission line FWHM. Since our estimate of the flux density at 2 keV is ~ 270 times larger than the value used by Lawrence et al. (from Rigopoulou, Lawrence, & Rowan-Robinson 1996), we find a value of $\alpha_{\text{ix}} \approx 1.2$, smaller by 0.8 than the value inferred by Lawrence et al., which moves Mrk 231 into line with the bulk of strong Fe II emitters in their sample. Furthermore, the expected hard X-ray luminosity from the cor-

relation between broad H α and 2–10 keV emission (Ward et al. 1988), using the H α flux measured by Smith et al. (1995; uncorrected for extinction), is $L_{\text{X}} \geq 2 \times 10^{44}$ ergs s^{-1} , in excellent agreement with the inferred X-ray luminosity.

5. SUMMARY

A moderately long ASCA observation of the infrared-luminous galaxy Mrk 231 shows a very flat hard X-ray spectrum, which strongly suggests that the central AGN is hidden behind a Compton-thick screen and is observed in X-rays only by scattering and reflection of the radiation into our line of sight. The inferred X-ray luminosity in the 0.5–10 keV band is $L_{\text{X}} \approx 2 \times 10^{44}$ ergs s^{-1} for a scattering fraction $f_{\text{sc}} \approx 1\%$, the value expected from the absorbing column density inferred from the X-ray spectrum. This is much larger than previous estimates, and the resulting ratio of $L_{\text{X}}/L_{\text{bol}}$ is typical of luminous Seyfert 1 galaxies and radio-quiet QSOs, indicating that the AGN dominates the bolometric luminosity of the galaxy and confirming the suggestion of Smith et al. (1995) that Mrk 231 is most properly classified as a low-ionization BAL QSO. The increase in the inferred X-ray luminosity over previous estimates also puts Mrk 231 in line with the correlations between the 2 keV– $1 \mu\text{m}$ spectral index and both the Fe II emission strength and the emission line FWHM found by Lawrence et al. (1997) for AGNs with extremely strong Fe II emission.

P. R. M. is supported by the NSF under grant AST 99-00871 and by the NASA Astrophysical Theory Program under grant NAG5-4061. C. S. R. appreciates support from Hubble Fellowship grant HF-01113.01-98A. This grant was awarded by the Space Telescope Institute, which is operated by the Association of Universities for Research in Astronomy, Inc., for NASA under contract NAS5-26555. C. S. R. also appreciates support from NASA under LTSA grant NAG5-6337 and the NSF under grants AST 95-29170 and AST 98-76887. We are grateful to Mike Nowak for producing Figure 3.

REFERENCES

- Boksenberg, A., Carswell, R. F., Allen, D. A., Fosbury, R. A. E., Penston, M. V., & Sargent, W. L. W. 1977, MNRAS, 178, 451
 DeGrijp, M. H. L., Keel, W. C., Miley, G. K., Goudfrooij, P., & Lub, J. 1992, A&AS, 96, 389
 Dermer, C. D., Bland-Hawthorn, J., Chiang, J., & McNaron-Brown, K. 1997, ApJ, 484, L121
 Elvis, M., et al. 1994, ApJS, 95, 1
 Genzel, R., et al. 1998, ApJ, 498, 579
 Iwasawa, K. 1999, MNRAS, 302, 96
 Iwasawa, K., & Comastri, A. 1998, MNRAS, 297, 1219
 Iwasawa, K., Fabian, A. C., & Matt, G. 1997, MNRAS, 289, 443
 Krolik, J. H., & Kallman, T. R. 1987, ApJ, 320, L5
 Krolik, J. H., Madau, P., & Życki, P. T. 1994, ApJ, 420, L57
 Lawrence, A., Elvis, M., Wilkes, B. J., McHardy, I., & Brandt, N. 1997, MNRAS, 285, 879
 Matt, G., Brandt, W. N., & Fabian, A. C. 1996, MNRAS, 280, 823
 Melnick, J., & Mirabel, I. F. 1990, A&A, 231, L19
 Rieke, G. H. 1988, ApJ, 331, L5
 Rigopoulou, D., Lawrence, A., & Rowan-Robinson, M. 1996, MNRAS, 278, 1049
 Sanders, D. B., & Mirabel, I. F. 1996, ARA&A, 34, 749
 Sanders, D. B., Soifer, B. T., Elias, J. H., Madore, B. F., Matthews, K., Neugebauer, G., & Scoville, N. Z. 1988, ApJ, 325, 74
 Smith, P. S., Schmidt, G. D., Allen, R. G., & Angel, J. R. P. 1995, ApJ, 444, 146
 Soifer, B. T., et al. 1984, ApJ, 278, L71
 Sturm, E., et al. 1996, A&A, 315, L133
 Turner, T. J. 1999, ApJ, 511, 142
 Vignati, P., et al. 1999, A&A, 349, L57
 Ward, M. J., Done, C., Fabian, A. C., Tennant, A. F., & Shafer, R. A. 1988, ApJ, 324, 767